Basis Functions for Axisymmetric Shell Elements Which Satisfy Rigid-Body Requirements

G. R. Heppler,* I. Sharf,† and J. S. Hansen‡
University of Toronto, Ontario, Canada

Shell elements are formulated using basis functions which are determined from the condition that the basis functions must reproduce all six rigid-body motions as a minimal requirement. As such the basis functions will in general not be polynomials; therefore the question of numerical integration schemes for the elements is also addressed. In order to demonstrate this capbility, examples are presented for a wide range of axisymmetric shells. For these problems, the appropriate basis functions are developed and the formulation is verified by tests that include eigenvalue, prescribed rigid-body motion, and load-deflection results.

Introduction

In a previous paper,[1] a method was developed which enabled shell-coordinate finite elements to reproduce exactly all six Cartesian rigid body modes. This was accomplished by forcing the rigid-body capability as an essential requirement for the derivation of the basis functions. The work in Ref. 1 presents the general approach to the problem; however, this method was only implemented for shells of revolution with straight meridians. The present work extends the previous results to the more general situation of arbitrary shells of revolution. Previous research that addressed the rigid-body motion capabilities of shell elements[2-11] was reviewed in Ref. 1; further, the merits of various approaches to this problem were also discussed. In addition to the above, a recently developed element[12] treats the question in a novel manner by employing shell coordinates but at the same time allowing the nodal degrees of freedom to be expressed relative to a Cartesian frame. The geometric representation achieved with this element is only exact for certain shell configurations (the complete set of conic sections among them), and in other cases matches the exact geometry at a finite number of defining points.

Element Formulation

The element to be discussed herein follows that presented in Ref. 1; thus the formulation will only be outlined in order to maintain completeness and for the readers' convenience. Reference should be made to Ref. 1 for further details.

The work is based on an extension of Reissner[13-16] and Mindlin[17] plate theory expressed in curvilinear shell coordinates. These theories have been shown to yield good results for thin to moderately thick shells.[18-24] In this work, linear strain-displacement relations of the form

$$\epsilon_{xx}=\frac{1}{\alpha}\left[\frac{\partial u}{\partial x}+\frac{v}{\beta}\frac{\partial \alpha}{\partial y}+w\frac{\partial \alpha}{\partial z}\right] \tag{1}$$

$$\epsilon_{yy}=\frac{1}{\beta}\left[\frac{\partial v}{\partial y}+\frac{u}{\alpha}\frac{\partial \beta}{\partial x}+w\frac{\partial \beta}{\partial z}\right] \tag{2}$$

$$\gamma_{xy}=\frac{1}{\beta}\frac{\partial u}{\partial y}+\frac{1}{\alpha}\frac{\partial v}{\partial x}-\frac{v}{\alpha\beta}\frac{\partial \beta}{\partial x}-\frac{u}{\alpha\beta}\frac{\partial \alpha}{\partial y} \tag{3}$$

$$\gamma_{yz}=\frac{\partial v}{\partial z}+\frac{1}{\beta}\frac{\partial w}{\partial y}-\frac{v}{\beta}\frac{\partial \beta}{\partial z} \tag{4}$$

$$\gamma_{zx}=\frac{\partial u}{\partial z}+\frac{1}{\alpha}\frac{\partial w}{\partial x}-\frac{u}{\alpha}\frac{\partial \alpha}{\partial z} \tag{5}$$

are used, where (x,y,z) are orthogonal curvilinear coordinates; where x and y lie at the midsurface of the shell, and z is normal to the midsurface. The tangential displacements, u and v, are in the x and y directions, respectively; w is the normal displacement; and α and β the Lamé coefficients. The normal strain ϵ_{zz} has not been included in the preceding equations in anticipation of the requirements of the Reissner/Mindlin formulation.

So that the present results are not restricted to thin, shallow shells, the factors $1/\alpha$ and $1/\beta$ are expanded in binomial series truncated to terms of $O(z^2)$. Thus the strain-displacement relations take the form

$$\epsilon=[B_0+zB_1+z^2B_2]\,d=\sum_{i=0}^{2}B_iz^i d \tag{6}$$

where $d=[\bar{u},\ \bar{v},\ \bar{w},\ \psi_x,\ \psi_y]^T$. As a result of the Reissner/Mindlin formulation, the displacement field is taken as

$$u(x,y,z)=\bar{u}(x,y)+z\psi_x(x,y) \tag{7}$$

$$v(x,y,z)=\bar{v}(x,y)+z\psi_y(x,y) \tag{8}$$

$$w(x,y,z)=\bar{w}(x,y) \tag{9}$$

Here, $\bar{u}$, $\bar{v}$ are midsurface displacements while $\bar{w}$ is a measure of the normal displacement and ψ_x, ψ_y are rotation measures.

The material is assumed to be linear-elastic, isotropic, and homogeneous; in the constitutive relation a shear correction factor ($k^2=5/6$) is included consistent with Reissner's development.[13] The formulation of the element stiffness matrices then follows directly, yielding

$$K=\int_v[N]^T\left[\sum_{i=0}^{2}B_iz^i\right]^T[D]\left[\sum_{j=0}^{2}B_jz^j\right][N]\,dV \tag{10}$$

where for a general shell $dV=\alpha\beta dx dy dz$ and $[N]$ is a matrix of basis functions. The basis functions are used to model the

Received Jan. 24, 1985; presented as Paper 85-0765 at the 26th AIAA/ASME/ASCE/AHS Structures, Structural Dynamics, and Materials Conference, Orlando, FL, April 15-17 1985; revision received May 20, 1985.

*Presently Assistant Professor, Systems Design Engineering, University of Waterloo, Waterloo, Ontario, Canada.
†Research Assistant, Institute for Aerospace Studies.
‡Professor, Institute for Aerospace Studies.

shell degrees of freedom ($\bar{u}$, $\bar{v}$, $\bar{w}$, ψ_x, ψ_y) in the form

$$\zeta = \sum_{i=1}^{m} N_i(x,y)\zeta_i \tag{11}$$

where ζ represents any of the shell degrees of freedom. When evaluating the stiffness matrix Eq. (10), exact integration through the thickness is used although terms of $O(z^3)$ and greater in the integrand are neglected.

Basis Functions

The kinematic relations between the shell coordinate degrees of freedom and the six possible rigid-body degrees of freedom, referenced to some convenient Cartesian frame, can be expressed in general by[1,4]

$$d = T(x,y)\delta \tag{12}$$

where d is the vector of shell degrees of freedom ($\bar{u}$, $\bar{v}$, $\bar{w}$, ψ_x, ψ_y), and δ a vector of rigid-body translations and rotations. The three rigid-body translations are designated by ($\delta_x,\delta_y,\delta_z$) and are parallel to the X, Y, and Z axes of the reference Cartesian frame, respectively. The three rotations are about the X, Y, and Z axes represented by ($\theta_x,\theta_y,\theta_z$). The transformation T is generally a function of the shell coordinates (x,y), see Fig. 1.

For the development of the basis functions, the elements are restricted to be rectangular with the curvilinear coordinates (x,y) coincident with lines of principal curvature. This choice allows the trail function to be expressed as

$$\zeta = \sum_{i=1}^{m}\sum_{j=1}^{n} \zeta_{ij} G_i(x) H_j(y) \tag{13}$$

where ζ_{ij} is the value of ζ at the ijth of the $m \times n$ nodes and $G_i(x)$, $H_j(y)$ are basis functions to be determined. The same procedure, previously outlined for shells with straight meridians, was followed for this more general case. Referring to Fig. 1 the kinematic transformation matrix of Eq. (12)

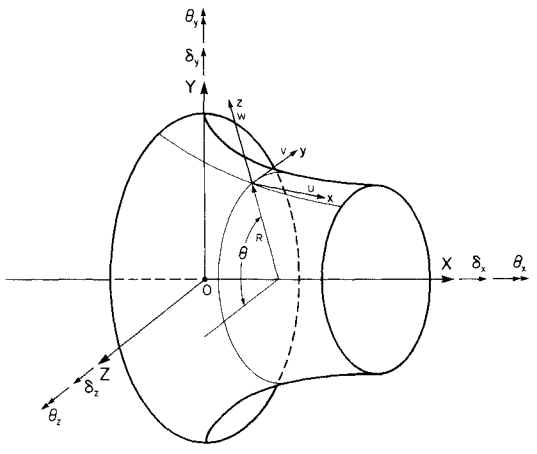

Fig. 1 Geometry of a shell of revolution.

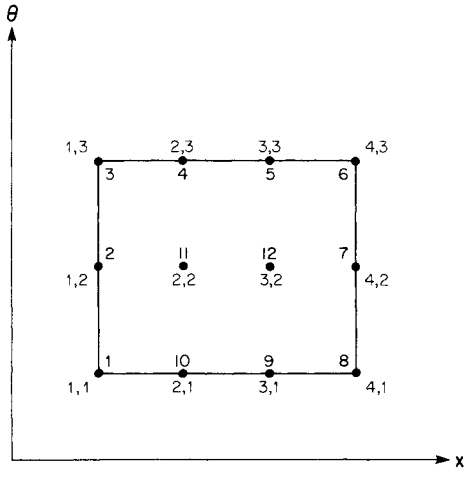

Fig. 2 Finite element for shells of revolution.

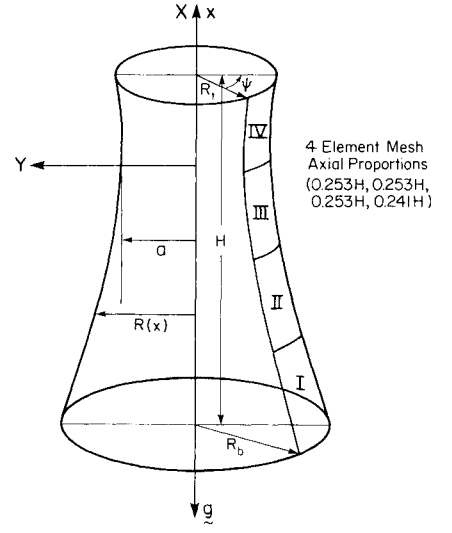

Geometric Data	Defining Equation	Material Data
R_t = 937.2 in.	$\left(\frac{Y}{a}\right)^2 - \left(\frac{X}{b}\right)^2 = 1$	E = 3.0 x 10^6 psi
R_b = 1540.7 in.		ν = 0.2
X_t = 962.88 in.	a = 843.48 in.	ρg = 0.08681 lb/in^3
X_b = -3038.76 in.	b = 1988.0 in.	
h = 6.0 in.		
ψ = 1.0 rad.		

Fig. 3 Hyperboloid cooling tower: geometry.

Table 1 Eigenvalues of representative elements from each geometry

No.	Hyperboloid cooling tower	Ogival shell		Parabolic dome
		Large element	Small element	
1	-1.0802×10^{-6}	-3.4724×10^{-8}	-2.9384×10^{-8}	-4.6093×10^{-7}
2	-4.5069×10^{-7}	-2.3217×10^{-8}	-1.4916×10^{-8}	-3.3334×10^{-7}
3	-3.0591×10^{-7}	-1.3411×10^{-7}	5.3011×10^{-9}	-6.2194×10^{-8}
4	8.9539×10^{-8}	-7.1783×10^{-9}	9.7667×10^{-9}	6.4450×10^{-8}
5	6.1092×10^{-7}	-3.9376×10^{-11}	1.3352×10^{-8}	2.8427×10^{-7}
6	1.1509×10^{-6}	2.8372×10^{-6}	1.0419×10^{-7}	1.1465×10^{-6}
7	2.5472×10^{3}	5.8950×10^{3}	9.9938×10^{3}	1.0928×10^{4}
8	8.0893×10^{3}	6.6265×10^{3}	1.8662×10^{4}	1.4851×10^{4}
9	9.2763×10^{3}	3.3137×10^{4}	2.5423×10^{4}	5.1207×10^{4}
10	1.0622×10^{4}	1.0271×10^{5}	2.6860×10^{4}	2.1176×10^{5}

is given specifically as[4]

$$\begin{bmatrix} \bar{u} \\ \bar{v} \\ \bar{w} \\ \psi_x \\ \psi_y \end{bmatrix} = \begin{bmatrix} \frac{1}{A} & \frac{R'}{A}\sin\theta & \frac{R'}{A}\cos\theta & 0 & \frac{(R-xR')}{A}\cos\theta & \frac{-(R-xR')}{A}\sin\theta \\ 0 & \cos\theta & -\sin\theta & -R & x\sin\theta & x\cos\theta \\ \frac{-R'}{A} & \frac{1}{A}\sin\theta & \frac{1}{A}\cos\theta & 0 & \frac{-(x+RR')}{A}\cos\theta & \frac{(x+RR')}{A}\sin\theta \\ 0 & 0 & 0 & 0 & \cos\theta & -\sin\theta \\ 0 & 0 & 0 & \frac{-1}{A} & \frac{-R'}{A}\sin\theta & \frac{-R'}{A}\cos\theta \end{bmatrix} \begin{bmatrix} \delta_x \\ \delta_y \\ \delta_z \\ \theta_x \\ \theta_y \\ \theta_z \end{bmatrix} \tag{14}$$

In the preceding relations $R=R(x)$ is the radius of the shell of revolution at any axial station and the primes denote differentiation with respect to x.

For a shell of revolution the Lamé parameters and the radii of curvature are given as[4]

$$A=[1+(R')^2]^{1/2}, \quad B=R \tag{15}$$

$$R_x=[1+(R')^2]^{3/2}/R'', \quad R_y=AR \tag{16}$$

Note that for this definition of A the x coordinate is not curvilinear at the midsurface of the shell, but axial and parallel to the axis of the shell. The coordinate θ replaces y due to the definition of B. Since (x,θ) are orthogonal coordinates, these may be considered to take the roles of (x,y) in Eq. (13). Because the shell in question is a surface of revolution, the basis functions corresponding to the θ direction are the same as those developed by Hansen and Heppler[1] which have been shown to allow the satisfaction of the rigid-body requirements of a specific axial cross section of the shell (i.e., $x=x_0=\text{const}$). Therefore the trial function will have a minimum of three nodes in the circumferential direction and the corresponding basis functions[1] are

$$H_1(\theta)=\frac{\sin(\theta-\theta_2)-\sin(\theta-\theta_3)+\sin(\theta_2-\theta_3)}{\sin(\theta_1-\theta_2)-\sin(\theta_1-\theta_3)+\sin(\theta_2-\theta_3)}$$

$$H_2(\theta)=\frac{\sin(\theta-\theta_3)-\sin(\theta-\theta_1)+\sin(\theta_3-\theta_1)}{\sin(\theta_2-\theta_3)-\sin(\theta_2-\theta_1)+\sin(\theta_3-\theta_1)}$$

$$H_3(\theta)=\frac{\sin(\theta-\theta_1)-\sin(\theta-\theta_2)+\sin(\theta_1-\theta_2)}{\sin(\theta_3-\theta_1)-\sin(\theta_3-\theta_2)+\sin(\theta_1-\theta_2)} \tag{17}$$

It remains to determine the basis functions, $G_i(x)$. Considering any meridian of the shell (i.e., $\theta=\theta_0=\text{const}$) and examining the first row in Eq. (14), it follows that u is related to the rigid-body motions through three unique functions of x. Specifically,

$$f(x)=1/A, \quad g(x)=R'/A, \quad h(x)=(R-xR')/A \tag{18}$$

Thus, in order that the $G_i(x)$ be able to reproduce a rigid-body motion, they must be able to reproduce the forms of f, g, and h. For an arbitrary rigid body motion it must follow that

$$\bar{u}(x,\theta_j)=\sum_{i=1}^{4}\bar{u}_{ij}G_i(x)H_j(\theta_j)=f\delta_x+gS_j\delta_y + gC_j\delta_z+hC_j\theta_y-hS_j\theta_z, \quad j=1,3 \tag{19}$$

where S_j and C_j are sine and cosine evaluated at $\theta=\theta_j$, respectively, and $\bar{u}_{ij}$ is the value of $\bar{u}$ at node ij such that

$$\bar{u}_{ij}=f_i\delta_x+g_iS_j\delta_y+g_iC_j\delta_z+h_iC_j\theta_y-h_iS_j\theta_z, \quad i=1,4 \tag{20}$$

In the above expression (f_i, g_i, h_i) are the functions (f, g, h) evaluated at $x=x_i$. Replacing $\bar{u}_{ij}$ in Eq. (19) with the explicit form from Eq. (20) and equating the coefficients of the rigid-body components results in an overspecified system of equations in terms of the unknowns $G_i(x)$ (five equations in four unknowns). Two equations can be shown to be linearly dependent on the other three and, hence, can be removed from the system. Then after adding the requirement that the $G_i(x)$ be normalized such that the sum of the basis functions add to one, the following system results (after removal of common constants from each side of the equation),

$$\begin{bmatrix} 1 & 1 & 1 & 1 \\ f_1 & f_2 & f_3 & f_4 \\ g_1 & g_2 & g_3 & g_4 \\ h_1 & h_2 & h_3 & h_4 \end{bmatrix} \begin{bmatrix} G_1 \\ G_2 \\ G_3 \\ G_4 \end{bmatrix} = \begin{bmatrix} 1 \\ f(x) \\ g(x) \\ h(x) \end{bmatrix} \tag{21}$$

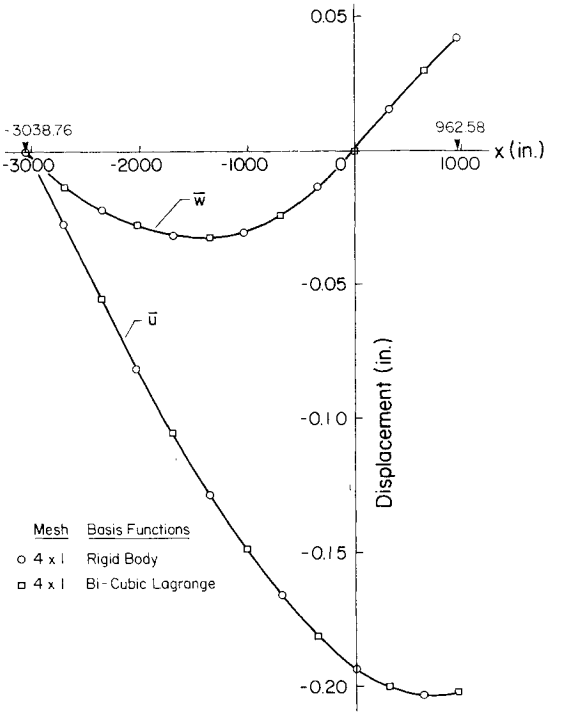

Fig. 4 Hyperboloid cooling tower: displacements $\bar{u}$, $\bar{w}$.

Therefore, when (f,g,h) are linearly independent, four unique basis functions will exist and four nodes are required in the x direction. It may occur that (f,g,h) are not linearly independent, in which case an alternate treatment is necessary; this is discussed in the example problems. Equation (21) can be solved for $G_i(x)$, $i=1,4$. Specifically, it can be shown that

$$G_1 = \{ (f-f_2)[(g_2-g_3)(h_2-h_4)-(h_2-h_3)(g_2-g_4)] + (g-g_2)[(h_2-h_3)(f_2-f_4)-(f_2-f_3)(h_2-h_4)] + (h-h_2)[(f_2-f_3)(g_2-g_4)-(g_2-g_3)(f_2-f_4)] \}/\Delta \quad (22a)$$

$$\Delta = \{ (f_1-f_2)[(g_2-g_3)(h_2-h_4)-(h_2-h_3)(g_2-g_4)] + (g_1-g_2)[(h_2-h_3)(f_2-f_4)-(f_2-f_3)(h_2-h_4)] + (h_1-h_2)[(f_2-f_3)(g_2-g_4)-(g_2-g_3)(f_2-f_4)] \} \quad (22b)$$

Basis functions $G_2(x)$, $G_3(x)$, and $G_4(x)$ may be found by cyclic permutation of the subscripts in the preceding equations. With reference to Fig. 2, the complete basis functions for $\bar{u}$ will be given by

$$N_1 = G_1(x)H_1(\theta) \quad N_2 = G_1(x)H_2(\theta) \quad N_3 = G_1(x)H_3(\theta)$$

$$N_4 = G_2(x)H_3(\theta) \quad N_5 = G_3(x)H_3(\theta) \quad N_6 = G_4(x)H_3(\theta)$$

$$N_7 = G_4(x)H_2(\theta) \quad N_8 = G_4(x)H_1(\theta) \quad N_9 = G_3(x)H_1(\theta)$$

$$N_{10} = G_2(x)H_1(\theta) \quad N_{11} = G_2(x)H_2(\theta) \quad N_{12} = G_3(x)H_2(\theta) \quad (23)$$

The above basis functions can reproduce all six rigid-body motions and will not induce strain in the shell element under a rigid-body motion. All of the degrees of freedom are of class C^0 across the element boundaries.

In the foregoing development, only the $\bar{u}$ degree of freedom has been dealt with specifically. The other degrees of freedom may be treated in a similar manner, but the following observations are in order. For modeling ease, it was decided that all of the degrees of freedom ($\bar{u}$, $\bar{v}$, $\bar{w}$, ψ_x, ψ_y) should be specified at the same nodes. Thus, every node will have the same number of degrees of freedom associated with it. Therefore, basis functions of the form developed for $\bar{u}$ are required for each of the remaining degrees of freedom. Note that the form of the G_i's is completely general for f, g, and h that are linearly independent. Then, by inspection of Eq. (14), it can be found that for $\bar{w}$

$$f=1/A, \quad g=R'/A, \quad h=(x+RR')/A \quad (24)$$

For $\bar{v}$ only two functional forms involving x are present in Eq. (14), but in order to have $\bar{v}$ specified at four nodes in the x direction, a third functional form was required. In order to achieve some symmetry this was selected to be the form of h as given below. Then for $\bar{v}$

$$f=x, \quad g=R, \quad h=xR \quad (25)$$

Note that this choice does not eliminate the capability of reproducing rigid-body motion.

Following an argument similar to that for $\bar{v}$ above, the choices of (f,g,h) for ψ_x and ψ_y were taken to be the same as those for $\bar{u}$. In summary, the selected basis functions have been formulated to allow recovery of all rigid-body motions if required; these basis functions are defined, through the definitions of (f,g,h), in terms of fundamental geometric descriptors of the shell.

Numerical Integration

Exact integration in the θ direction is achieved by the method given in Ref. 1 and, for the examples to be presented in this paper, seventh-order Gauss quadrature was found to be satisfactory in the x direction. This relatively high order of integration (seven) was required in order to integrate the longitudinal basis functions accurately and achieve six strong zero eigenvalues. Relaxing the integration order below seven was found to lead to the loss of one or more of the rigid-body modes for these geometries.

Numerical Tests and Results

Three shell geometries were employed to assess the above element. They were a hyperboloid cooling tower, an ogival cylinder, and a parabolic dome. In each case an eigenvalue analysis was performed along with a specified rigid-body motion in a gravitational field where the calculated work is compared to the theoretical work. In addition, the consistent internal force vector was calculated for each of the six possible rigid-body motions and, finally, a problem with specified boundary constraints and applied load was treated and compared to previous results.

Hyperboloid Cooling Tower

The geometry and material properties of the cooling tower are shown in Fig. 3. This geometry has the following expression for the radius:

$$R(x) = a\sqrt{(x/b)^2+1} \quad (26)$$

Then from Eqs. (15), (16), and (26) all of the geometric parameters in the strain-displacement relations, Eqs. (1-5) and (9), may be determined in addition to the basis functions, thus allowing formation of the element stiffness matrix.

The results of an eigenvalue analysis on the stiffness matrix for element number I in Fig. 3 is given in Table 1 where the first ten eigenvalues are listed. Notice that the first six eigenvalues are at least nine orders of magnitude less than the seventh eigenvalue. The first three eigenvalues are negative as a result of the numerical errors that arise in the eigenvalue calculation and the magnitude of these numbers reflects the accuracy of the eigenvalue calculation because the stiffness matrix is necessarily positive semidefinite. Hence, as required, there are six "zero" eigenvalues present.

A further test used to assess the basis functions involved their use in forming the consistent force vector associated with the body forces arising from gravitational acceleration. The test consisted of specifying a unit rigid-body displacement in the Cartesian reference frame in the presence of a uniform gravitational acceleration, not necessarily directed in the same direction as the prescribed unit displacement. The work calculated from the dot product of the displacement vector and the calculated gravitational consistent force vector was compared to the exact work calculated analytically. Results are given in Table 2. For the cooling tower example the error in the calculated work done is uniformly less than 1% for the two orientations of the gravitational acceleration vector investigated. It is also illustrated that there is no benefit obtained in increasing the integration order in the x direction from seventh- to ninth-order Gaussian quadrature.

The stiffness matrix is evaluated in the next test in which the force vector arising from the multiplication of the stiffness matrix and a specified displacement vector is calculated under a set of prescribed rigid-body motions. The stiffness matrix for element I, shown in Fig. 3, was multiplied by six displacement vectors in turn. These displacement vectors corresponded to each of the six fundamental rigid-body motions (δ_x, δ_y, δ_z, θ_x, θ_y, θ_z). See Table 3. In all cases the resulting vector was "numerically zero," by which we mean that all

entries were $O(10^{-8})$ or less. By comparison, entries in the stiffness matrix were $O(10^5)$ and the nonzero entries in the displacement vectors were $O(10^{-2})$ or greater. The norms of the prescribed as well as calculated vectors and matrices are given in Table 3, where the vector norm is the Euclidian norm and the corresponding matrix norm is given by (largest eigenvalue of $K^TK)^{1/2}$ (Ref. 27). These values serve to further illustrate that the calculated force vector is "numerically zero."

Finally, for this example the results of calculations corresponding to a gravity self-weight loaded cooling tower are presented (Fig. 3). Comparison is made to results obtained by employing the element developed in Ref. 24 which is identical to that developed herein except that bicubic Lagrange basis functions were used in the element formulation. There were 195 degrees of freedom present in the model that used the rigid-body basis functions developed herein, while the model comprised of the bicubic Lagrange basis function elements had 260 degrees of freedom.

In keeping with the axisymmetric nature of the loading, there was no circumferential variation in the computed displacements in either case with $\bar{v}$ and ψ_y being uniformly zero everywhere. The meridional and normal displacements are given in Fig. 4 where the difference between the results obtained with the two different types of basis functions is indistinguishable.

In Fig. 5 the stress resultants are compared not only to those from the bicubic Lagrange element[24] but also to those reported by Fonder and Clough,[5] where explicit rigid-body augmentation was not employed for this example. The agreement between the present element and that of Ref. 24 is again excellent while the agreement to the results from Ref. 5, where 252 degrees of freedom were used, is also very good.

The moment resultants are presented in Fig. 6. The differences in the manner in which the two types of basis functions approximate the displacement field are apparent in this figure. Although both elements yielded similar trends there were instances of large disagreement between the two sets of results, particularly near the base of the tower ($x = -3038.76$ in.). There is also an absence of "near continuity" across element boundaries in both cases. For the moment resultant data there is no clear "best choice" of basis functions.

Ogival Cylinder

This shell is formed by rotating a segment of a circular arc about an axis that lies between the generating curve and its center of curvature. The geometry for the present problem is

Table 2 Work done by a prescribed unit rigid-body translation in a gravitational field

Geometry	Direction cosine of g in (X,Y,Z)	Analytical work, lb-in.	Numerical work, lb.-in.	Δ%
Hyperboloid cooling tower, $h=0.5$ in.:				
Seventh-order Gauss, $\delta_x=1$	(1, 0, 0)	34,994	35,214	0.6
Seventh-order Gauss, $\delta_x=1$	$\left(\frac{1}{\sqrt{3}}, \frac{-1}{\sqrt{3}}, \frac{1}{\sqrt{3}}\right)$	20,204	20,330	0.6
Ninth-order Gauss, $\delta_x=1$	$\left(\frac{1}{\sqrt{3}}, \frac{-1}{\sqrt{3}}, \frac{1}{\sqrt{3}}\right)$	20,204	20,331	0.6
Ogival shell:				
$\delta_x=1$	$\left(\frac{1}{\sqrt{2}}, \frac{1}{\sqrt{2}}, 0\right)$	185.53	185.54	0
$\delta_z=1$	$\left(\frac{1}{\sqrt{2}}, \frac{1}{\sqrt{2}}, 0\right)$	0	5.3291×10^{-14}	0
Parabolic dome:				
$\delta_x=1$	(−1, 0, 0)	−2875.2	−3031.3	5
$\delta_y=1$	(−1, 0, 0)	0	1.3145×10^{-12}	0

Table 3 Prescribed motion results

Geometry	Stiffness matrix norm	Prescribed rigid-body motion vector	Corresponding nodal displacement vector norm	Calculated force vector norm
Hyperboloid cooling tower	1.05×10^{11}	(1,0,0,0,0,0)	3.46	5.40×10^{-8}
		(0,1,0,0,0,0)	3.46	2.09×10^{-7}
		(0,0,1,0,0,0)	3.46	1.67×10^{-7}
		(0,0,0,1,0,0)	3050.00	8.10×10^{-8}
		(0,0,0,0,1,0)	3270.00	2.36×10^{-7}
		(0,0,0,0,0,1)	2690.00	2.10×10^{-7}
Ogival shell	7.57×10^{11}	(1,0,0,0,0,0)	3.46	2.73×10^{-8}
		(0,1,0,0,0,0)	3.46	2.72×10^{-8}
		(0,0,1,0,0,0)	3.46	3.15×10^{-8}
		(0,0,0,1,0,0)	154.00	1.97×10^{-8}
		(0,0,0,0,1,0)	252.00	2.02×10^{-8}
		(0,0,0,0,0,1)	233.00	1.53×10^{-8}
Paraboloid shell	4.78×10^{10}	(1,0,0,0,0,0)	3.46	3.48×10^{-7}
		(0,1,0,0,0,0)	3.46	9.94×10^{-8}
		(0,0,1,0,0,0)	3.46	1.08×10^{-7}
		(0,0,0,1,0,0)	903.00	5.59×10^{-8}
		(0,0,0,0,1,0)	1080.00	1.94×10^{-7}
		(0,0,0,0,0,1)	842.00	1.23×10^{-7}

given, along with the material properties, in Fig. 7. The radius, as a function of the axial position x, is given by

$$R(x) = \sqrt{r^2 - [x - r\sin(\phi/2)]^2} + [b - r\cos(\phi/2)] \qquad (27)$$

Although the method outlined above for constructing basis functions that will admit rigid-body motions is quite general, this example illustrates that caution is advisable. In specifying the functions f, g, and h in Eqs. (18), (24), and (25) for use in creating the basis functions, it was required that f, g, and h be linearly independent and nonconstant. For the present geometry it can be shown that the (f,g,h) used to interpolate $\bar{u}$ and $\bar{w}$ [Eqs. (18) and (24)] are linearly dependent; hence, these choices are unacceptable. Two solutions to this problem are possible: first, reduce the number of nodes in the axial direction from four to three [to reflect the fact that only two of (f,g,h) are independent] or choose a new form for one of (f,g,h) which is linearly independent. The first option leads to a formulation that changes with shell geometry—an unattractive option. The second choice requires only minor changes to the computer code and leaves the form of the element intact. Hence for the ogival cylinder, (f,g,h) for degrees of freedom $(\bar{u},\bar{w},\psi_x,\psi_y)$ become

$$f = 1/A, \quad g = R'/A, \quad h = R'/A^2 \qquad (28)$$

and those for $\bar{v}$ remain as specified in Eq. (25).

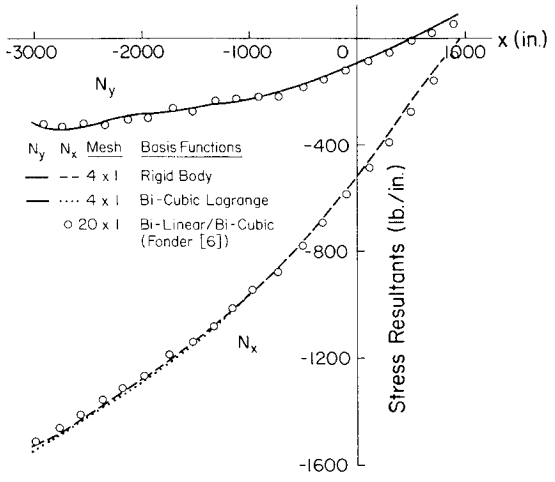

Fig. 5 Hyperboloid cooling tower: stress resultants, N_x, N_y.

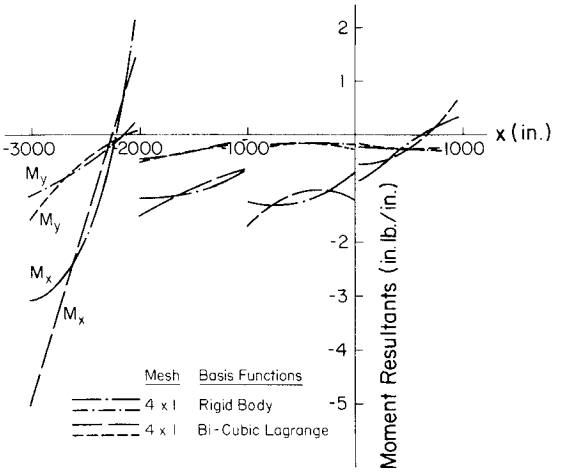

Fig. 6 Hyperboloid cooling tower: moment resultants, M_x, M_y.

The results of the eigenvalue analysis of the stiffness matrix are given in Table 1. The results for the "large element" are the eigenvalues of the stiffness matrix of an element which spans one radian of the arc and the entire height of the shell. The "small element" also covers one radian but only the bottom fifth of the height of the cylinder. As in the previous case there are the requisite six zero eigenvalues for both examples.

The accuracy achieved in the calculation of the work done in applying a unit translation, as compared to the exact value, is shown to be excellent with a negligible error being present, see Table 2.

As in the previous case, the internal force vectors calculated by taking the product of an element stiffness matrix and a prescribed displacement vector that corresponds to a fundamental rigid-body motion are "numerically zero." The pertinent vector norms are given in Table 3 and the relative magnitudes of the individual entries were similar to those given in the previous example.

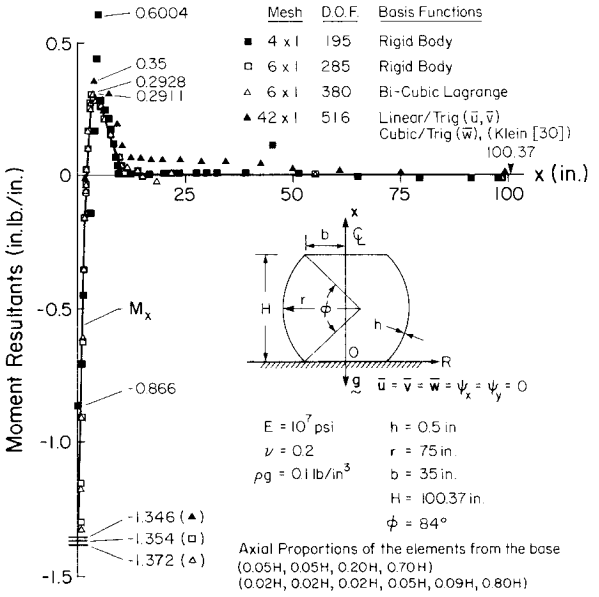

Fig. 7 Ogival shell: moment resultant, M_x.

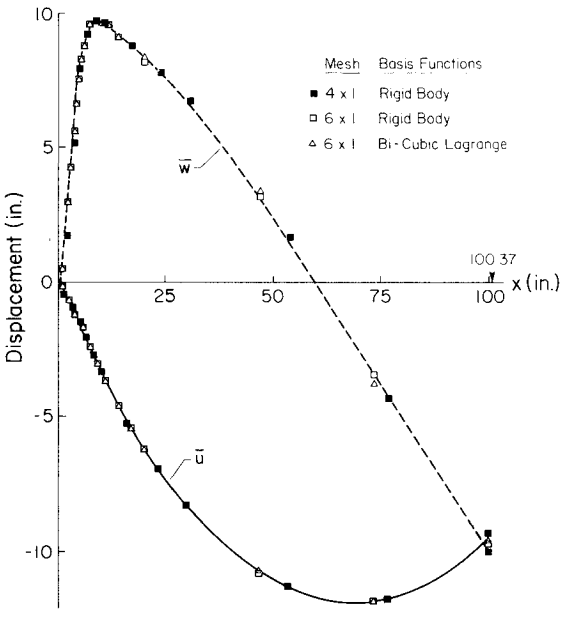

Fig. 8 Ogival shell: displacements, $\bar{u}$, $\bar{w}$.

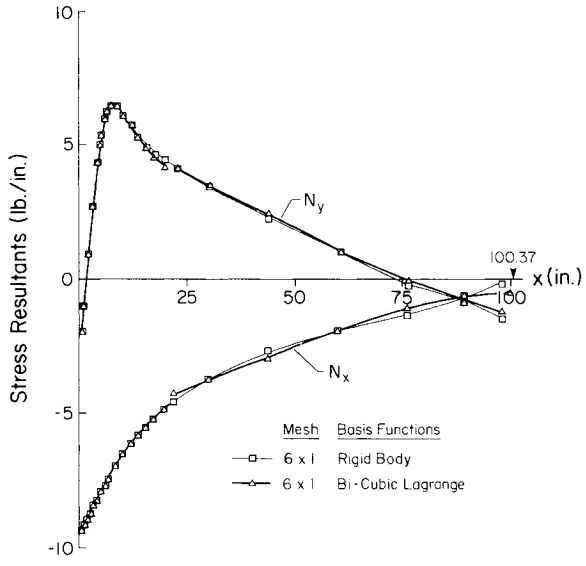

Fig. 9 Ogival shell: stress resultants, N_x, N_y.

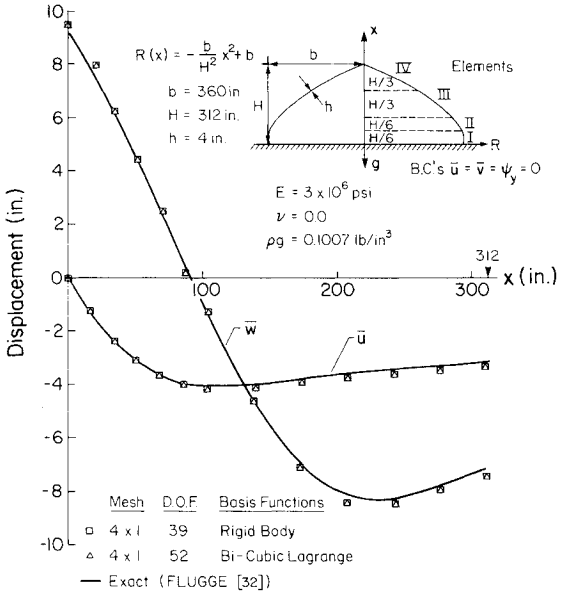

Fig. 10 Parabolic dome: displacements, $\bar{u}$, $\bar{w}$.

The results of loading the shell shown in Fig. 7 by gravity, in the direction shown, are presented in Figs. 7-9. Comparison is made to results obtained from a similar bicubic Lagrange element[24] and to more limited results due to Klein.[28] The meridional moment results are illustrated in Fig. 7, where the best results of Klein[28] are also included. It is evident that in order to achieve good moment resultant data, four elements are insufficient for this problem and six elements based on either the present rigid-body or bicubic Lagrange basis functions yield superior results to the 42-element model of Ref. 30. The principal difference between the present results and those due to the bicubic Lagrange element appear at the two local maxima (Fig. 7), where the Lagrange element gives slightly lower values than the rigid-body element. This trend is also evident in the results for M_y.[29]

Although four elements did not provide a very good approximation to the moment resultants, it may be seen in Fig. 8 that, in terms of the displacements $\bar{u}$ and $\bar{w}$, four elements yield very good results. Only slight differences in the results

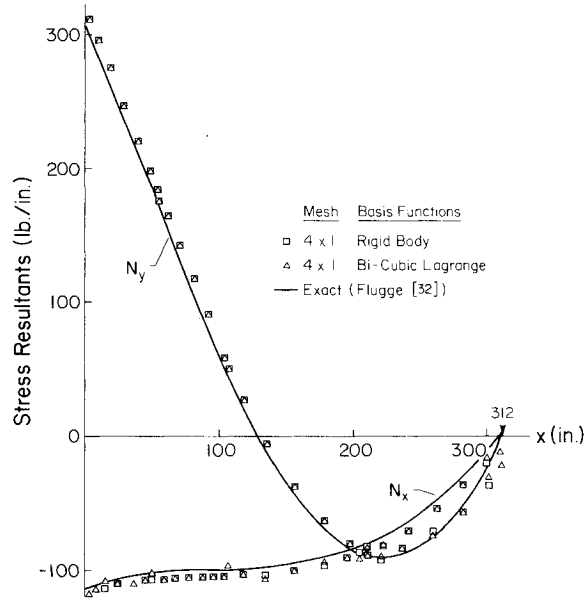

Fig. 11 Parabolic dome; stress resultants, N_x, N_y.

from the two types of basis functions are in evidence for $\bar{w}$.

Finally, the stress resultants for this problem are reported in Fig. 9 where the rigid-body element model exhibits superior interelement continuity of the stress resultants. The axial stress resultant N_x tends to zero more strongly at the top of the shell for the rigid-body basis functions than for the bicubic Lagrange basis functions. Otherwise, the agreement between the two sets of results is good.

Parabolic Dome

Unlike the previous two examples, the shell used in this example is closed to form a pointed dome (Fig. 10). Again loading will be due to gravity directed downward from the apex of the dome. The radius equation is

$$R(x) = -(b/H^2)x^2 + b \tag{29}$$

and the forms of (f,g,h) used for the hyperboloid example [Eqs. (18), (24), and (25)] are also used here.

As in the previous two examples there are the necessary six zero eigenvalues; with those reported in Table 1 corresponding to an element which spans one radian of arc and the entire height of the dome. The work done under a prescribed unit translation in a gravitational field is reported in Table 2 for an element that extends half-way up the dome from the base. The error in the calculated work is larger than in previously obtained results, i.e., ~5%. The exact reason for this large error has not been determined; the order of integration does not significantly affect the result.

The internal forces arising due to a prescribed rigid-body motion are again "numerically zero," with the results for this example being similar to the previous two cases; see Table 3.

The results for the gravity-loaded dome are given in Figs. 10 and 11. The differences in the displacement results (Fig. 10) cannot be distinguished in this figure with both types of basis functions yielding essentially identical results; both of which have very good agreement with the membrane theory results of Flügge.[30] Similarly there is little difference between the stress resultant values, Fig. 11, calculated by either the finite elements or membrane theory,[30] except that the rigid-body basis functions have a better interelement continuity of the stress resultants. The differences in the moment resultants are more pronounced,[29] particularly in the case of M_y.

Conclusions

A general method for constructing elements in shell coordinates that implicitly possess the capability of recovering all six rigid-body motion has been presented. It has been illustrated by several examples utilizing three very different shell geometries that the basis functions developed by the method presented herein yield excellent results, both in terms of accuracy and economy.

References

[1]Hansen, J. S. and Heppler, G. R., "A Mindlin Shell Element Which Satisfies Rigid Body Requirements," *AIAA Journal*, Vol. 22, Feb. 1985, pp. 288-295.

[2]Cantin, G. and Clough, R. W., "A Curved Cylindrical Shell, Finite Element," *AIAA Journal*, Vol. 6, June 1968, pp. 1057-1062.

[3]Cantin, G., "Rigid Body Motions in Curved Finite Elements," *AIAA Journal*, Vol. 8, July 1970, pp. 1252-1255.

[4]Dawe, D. J., "Rigid Body Motions and Strain-Displacement Equations of Curved Shell Finite Elements," *International Journal of Mechanical Science*, Vol. 14, 1972, pp. 569-578.

[5]Fonder, G. and Clough, R. W., "Explicit Addition of Rigid Body Motions in Curved Finite Elements," *AIAA Journal*, Vol. 11, March 1973, pp. 305-312.

[6]Cantin, G., "Rigid Body Motions and Equilibrium in Finite Elements," *Finite Elements for Thin Shells and Curved Members*, edited by D. G. Ashwell and R. H. Gallagher, John Wiley & Sons, London, 1976, pp. 55-62.

[7]Fonder, G. A., "Studies in Doubly Curved Elements for Shells of Revolution," *Finite Elements for Thin Shells and Curved Members*, edited by D. G. Ashwell and R. H. Gallagher, John Wiley & Sons, London, 1976, pp. 113-130.

[8]Gallagher, R. H., "Problems and Progress in Thin Shell Finite Element Analysis," *Finite Elements for Thin Shells and Curved Members*, edited by D. G. Ashwell and R. H. Gallagher, John Wiley & Sons, London, 1976, pp. 1-14.

[9]Morris, A. J., "A Summary of Appropriate Governing Equations and Functionals in the Finite Element Analysis of Thin Shells," *Finite Element for Thin Shells and Curved Members*, edited by D. G. Ashwell and R. H. Gallagher, John Wiley & Sons, London, 1976, pp. 15-40.

[10]Irons, B. M., "The Semi Loof Shell Element," *Finite Elements for Thin Shells and Curved Members*, edited by D. G. Ashwell and R. H. Gallagher, John Wiley & Sons, London, 1976, pp. 197-222.

[11]Ashwell, D. G., "Strain Elements with Applications to Arches, Rings and Cylindrical Shells," *Finite Elements for Thin Shells and Curved Members*, edited by D. G. Ashell and R. H. Gallagher, John Wiley & Sons, London, 1976.

[12]Moore, C. J., Yang, T. Y., and Anderson, D. C., "A New 48 D.O.F. Quadrilateral Shell Element with Variable Order Polynomial and Rational B Spline Geometries with Rigid Body Modes," *International Journal of Numerical Methods in Engineering*, Vol. 20, Nov. 1984, pp. 2121-2141.

[13]Reissner, E., "The Effect of Transverse Shear Deformation on the Bending of Elastic Plates," *Journal of Applied Mechanics, Transactions of ASME*, Vol. 12, June 1945, pp. A69-A77.

[14]Goodier, J. N., "Discussion of Ref. 13 in *Journal of Applied Mechanics, Transactions of ASME*, Vol. 68, Sept. 1946, pp. A249-A252.

[15]Reissner, E., "On Bending of Elastic Plates," *Quarterly of Applied Mathematics*, Vol. 5, No. 1, 1947, pp. 55-68.

[16]Green, A. E., "On Reissner's Theory of Bending of Elastic Plates," *Quarterly of Applied Mathematics*, Vol. 7, No. 2, 1949, pp. 223-228.

[17]Mindlin, R. D., "Influence of Rotary Inertia and Shear on Flexural Motions of Elastic Plates," *Journal of Applied Mechanics*, Vol. 18, March 1951, pp. 31-38.

[18]Ahmad, S., Irons, B. M., and Zienkiewicz, O. C., "Analysis of Thick and Thin Shell Structures by Curved Finite Elements," *International Journal of Numerical Methods in Engineering*, Vol. 2, 1970, pp. 419-451.

[19]Zienkiewicz, O. C., Taylor, R. L., and Too, J. M., "Reduced Integration Technique in General Analysis of Plates and Shells," *International Journal of Numerical Methods in Engineering*, Vol. 3, April-June 1971, pp. 275-290.

[20]Zienkiewicz, O. C. and Hinton, E., "Reduced Integration Function Smoothing and Non-Conformity in Finite Element Analysis (with Special Reference to Thick Plates)," *Journal of the Franklin Institute*, Vol. 302, Nov./Dec. 1976, pp. 443-461.

[21]Onate, E., Hinton, E., and Glover, N., "Techniques for Improving the Ahmad Shell Element," *2nd International Conference on Applications of Numerical Modeling*, Madrid, 1978, pp. 389-399.

[22]Pugh, E.D.L., Hinton, E., and Zienkiewicz, O. C., "A Study of Quadrilateral Plate Bending Elements with Reduced Integration," *International Journal of Numerical Methods in Engineering*, Vol. 12, July 1978, pp. 1059-1079.

[23]Hughes, T.J.R. and Cohen, M., "The Heterosis Finite Element for Plate Bending," *Computers and Structures*, Vol. 9, 1978, pp. 445-450.

[24]Heppler, G. R., "On the Analysis of Shell Structures Subjected to a Blast Environment: A Finite Element Approach," Ph.D. Thesis, University of Toronto, Canada, 1984.

[25]Vlasov, V. Z., "General Theory of Shells and Its Applications to Engineering," (Translation), NASA TT F-99, April 1964.

[26]Vlasov, V. S., "Basic Differential Equations in General Theory of Elastic Shells," NACA TM-1241, 1951.

[27]Noble, B., *Applied Linear Algebra*, Prentice-Hall, Englewood Cliffs, N.J., 1969.

[28]Klein, S., "A Study of the Matrix Displacement Method as Applied to Shells of Revolution," *Matrix Methods in Structural Mechanics*, edited by J. S. Przemieniecki, R. M. Bader, W. F. Bozich, J. R. Johnson, and W. J. Mykytow, AFFDL-TR-67-80, pp. 275-298.

[29]Heppler, G. R., Sharf, I., and Hansen, J. S., "Shell Elments Which Satisfy Rigid Body Requirements," *AIAA/ASME/AHS 26th Structures, Structural Dynamics and Materials Conference*, Orlando, FL, April 1985, pp. 550-560.

[30]Flügge, W., *Stresses in Shells*, Springer-Verlag, Berlin, 1962.